Carrier Synchronizator in Nonbinary LDPC Coded Modulation Systems

Qiang Zhang, Zhong-yang Yu, and Baoming Bai(✉)

State Key Laboratory of Integrated Service Networks, Xidian University, Xi'an, China
bmbai@mail.xidian.edu.cn

Abstract. This paper proposes carrier synchronizator in a nonbinary LDPC and high-order QAM system in order to solve some relevant problems (e.g. Doppler shift, spectrum efficiency etc.) in the satellite communication. The carrier synchronizator is divided into two parts: frequency estimator and phase estimator. The frequency estimator has two steps: single pilot block-based coarse frequency estimation and multiple pilot block-based fine frequency estimation performed by an autocorrelation (AC) operation and a cross-correlation (CC) operation, respectively. Through frequency compensation, the following phase estimator is carried out by the classical maximum likelihood (ML) criterion. Simulation results show that, for a (225, 173) nonbinary LDPC code over GF(16) with a 16-QAM systems, the proposed carrier synchronizator can eliminate large Doppler shift in the presence of random phase offset with low complexity.

Keywords: Pilot-aided · Nonbinary LDPC · High-order QAM
Carrier synchronization

1 Introduction

In recent years, satellite communication has been forced to develop rapidly due to the ever-growing demands for the space TT&C and the deep-space exploration [1–3]. There exist large Doppler shift and limited spectrum resource in the above communication fields. Thus, it is absolutely necessary to design an appropriate carrier synchronization strategy applied into a new coded modulation system.

The so-called carrier synchronization is a key one of the synchronization techniques [4, 5]. According to whether using the pilot (known to both transmitter and receiver) or not, carrier synchronizator can be classified as data-aided (DA)-type synchronizator and non-data-aided (NDA)-type synchronizator [6, 7]. In the satellite communication, synchronization time (including its acquisition and track) required is extremely short, which means that the former is more preferred. With the help of the pilot, one can perform the carrier synchronization much more rapidly. Further, DA-type synchronizator can be divided into auto-correlation (AC) synchronizator and cross-correlation (CC) synchronizator, where the classical L&R [8] belongs to the former and has wide estimation range with low complexity, while the popular cross-correlation [9] owns high accuracy. Specifically, under the conditions of the same signal-to-ratio (SNR) and

B. Li et al. (Eds.): ChinaCom 2017, LNICST 237, pp. 122–131, 2018.
https://doi.org/10.1007/978-3-319-78139-6_13

pilot overhead, the AC synchronizator has larger estimation range and lower complexity, while the CC synchronizator achieves higher estimation accuracy. Thus, a joint AC and CC synchronizator is proposed.

Especially with the development of modern coding technique, more and more researchers try to combine both the carrier synchronization and channel codes (e.g. LDPC etc.) [10, 11]. However, their studies focus on binary LDPC-based carrier synchronization. In recent years, nonbinary LDPC coding technique has been widely concerned because of its numerous advantages, especially for the short code lengths [12, 13]. Further, the coding technique is more suitable for the combination of high-order QAM technique, obtaining higher spectrum efficiency.

Based on our previous work [14], a novel carrier synchronizator is proposed in a nonbinary LDPC and high-order QAM system. We consider making estimation of frequency offset by two steps i.e. coarse frequency offset estimation based on single pilot blocks and fine frequency offset estimation based on multiple disjoint pilot blocks. Then, ML-based phase offset estimation will be carried out. Simulation results show that the proposed synchronizator can achieve asymptotically optimal performance as pilot overhead increases.

The remaining sections of this paper are structured as follows: The system model is introduced in Sect. 2. The detailed descriptions of our proposed carrier synchronizator are presented in Sect. 3. Sections 4 and 5 give some relevant simulation results and conclusions, respectively.

2 System Model

Figure 1 depicts a system model used in this paper. First, a data sequence is sent into an encoder to obtain corresponding check bits. Then, the resulting codeword and a pilot sequence can make up of a specific frame structure shown in Fig. 2 with the use of a multiplexer (MUX), where it has N pilot blocks, each having L_i symbols $(i = 1, 2, \ldots, N)$ and $N - 1$ data blocks, each having M_i symbols $(i = 1, 2, \ldots, N - 1)$. Next, the multiplexed signals are converted into complex baseband signals by a modulator (MOD) corresponding to the nonbinary LDPC code. In the satellite communication, the modulated signals are disturbed by large Doppler shift f_d $(|f_d T| \leq 0.5)$ and random phase offset θ $(\theta \in [-\pi, \pi)$ is constant per packet). Assume single carrier transmission in Gaussian noise (AWGN) channel with ideal symbol timing, the k-th received equivalent baseband signal can be expressed as

$$\begin{aligned} r(k) &= s(k)\exp[j(2\pi f_d T k + \theta)] + n(k) \\ k &= 1, 2, \ldots, \sum_{i=1}^{N} L_i + \sum_{i=1}^{N-1} M_i \end{aligned} \tag{1}$$

where T is the symbol duration, $s(k)$ is the normalized-energy modulation signal, $n(k) \sim \mathcal{CN}(0, N_0)$ is the circular symmetric complex Gaussian random variable, whose real and imaginary parts have variances $N_0/2$.

At receiver, the received pilot signals $\{r_p(k)\}$ from the demultiplexer (DEMUX) are first sent into the proposed carrier synchronizator (see Sect. 3 for details) to obtain corresponding estimates $\hat{f}_d$ and $\hat{\theta}$. Then, the received data signals $\{r_d(k)\}$ are corrected by the above estimates through a compensator (COM). Again passing through a demodulator (DEMOD) and a nonbinary LDPC decoder, the original data information can be recovered.

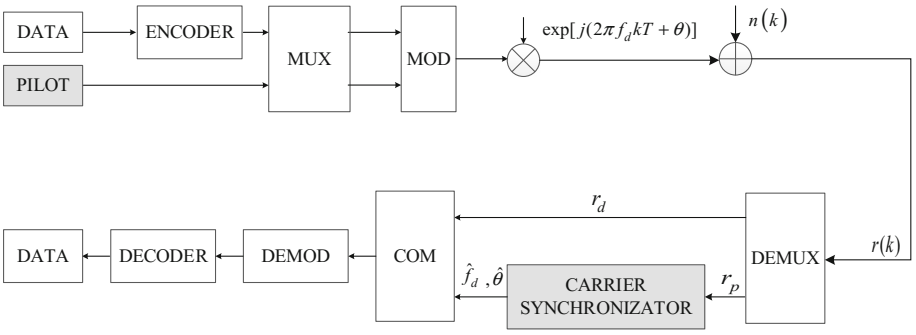

Fig. 1. System model

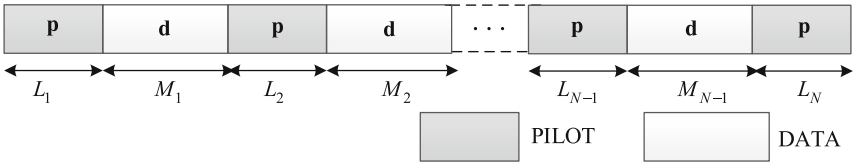

Fig. 2. Frame structure

3 Carrier Synchronizator

In this paper, the proposed carrier synchronizator is divided into two parts: one is a frequency estimator, and the other is a phase estimator. Further, the frequency estimator has two steps, i.e. coarse frequency estimation and fine frequency estimation performed by an auto-correlation (AC) operator and a cross-correlation (CC) operator respectively.

3.1 Coarse Frequency Estimation

In the coarse frequency estimation, we use the received signals corresponding to the first pilot block. First, a so-called removed-modulation operation is done by means of

$$\begin{aligned} z(k) &= r(k)s^*(k) \\ &= \exp[j(2\pi f_d Tk + \theta)] + v(k), k \in \kappa \end{aligned} \tag{2}$$

where $v(k) \triangleq n(k)\tilde{s}^*(k)$ is the noise signal, whose statistical characteristics are the same as $n(k)$. κ is the set of sampling instants corresponding to all the pilot signals, i.e. $\kappa = \{0, 1, \ldots, L_1 - 1, L_1 + M_1, \ldots, \sum_{i=1}^{N-1}(L_i + M_i), \ldots, \sum_{i=1}^{N-1}(L_i + M_i) + 1, \ldots, \sum_{i=1}^{N-1}(L_i + M_i) + L_N - 1\}$.

Next, a so-called autocorrelation operation is performed based on (2) with the form of

$$R_a(\alpha) = \frac{1}{L_1 - \alpha} \sum_{i=0}^{L_1 - 1 - \alpha} z^*(i) z(i + \alpha) \tag{3}$$

where α is the effective delay length with an empirical range from 1 to $L_1/2$ [8], L_1 is the length of the first pilot block.

Then, taking argument of (3) can get a coarse frequency estimate with the form of

$$\hat{f}_d^c = \frac{1}{2\pi\alpha T} \arg\{R_a(\alpha)\},\ \left|\hat{f}_d^1 T\right| \le \frac{1}{2\alpha}. \tag{4}$$

To estimate a larger frequency, letting the coefficient $\alpha = 1$ can yield

$$\hat{f}_d^{c1} = \frac{1}{2\pi T} \arg\{R_a(1)\},\ \left|\hat{f}_d^1 T\right| \le 0.5. \tag{5}$$

After frequency compensation, the classical L&R algorithm [8] is introduced to achieve a lower SNR threshold, resulting in another coarse frequency estimate

$$\begin{aligned} \hat{f}_d^{c2} &= \frac{1}{\pi T(N_c + 1)} \arg\left\{ \sum_{\alpha_1 = 0}^{N_c - 1} R_a(\alpha_1) \right\}, \\ \left|\hat{f}_d^{c2} T\right| &\le \frac{1}{N_c + 1} \end{aligned} \tag{6}$$

where N_c is the smoothing noise coefficient with an empirical value of $L_1/2$, $R_a(\alpha_1)$ is the weighted summation term corresponding to all the compensated removed-modulation signals with the form of

$$R_a(\alpha_1) = \frac{1}{L_1 - \alpha_1} \sum_{i=0}^{L_1 - 1 - \alpha_1} z_1^*(i) z_1(i + \alpha_1) \tag{7}$$

where $z_1(i) \triangleq z(i) \exp[-j(2\pi \hat{f}_d^{c1} T i)]$ is also the removed-modulation signal corrected by the preliminary frequency estimate $\hat{f}_d^{c1}$.

It is found through simulations that, for a small pilot block, the coefficient $N_c \approx L_1/3$; and for a relatively large one, the coefficient $N_c \approx L_1/2$, which is the same as the L&R algorithm.

Based on the above discussions, the coarse frequency estimator can be formulated as follows:

Initialization: set the initial frequency estimate $\hat{f}_d^c = 0$, the sampling instant $k \in \{1, 2, \ldots, L_1\}$.

(a) obtain the removed-modulation signal $z(k)$ according to (2);
(b) get the autocorrelation value $R_a(\alpha)|_{\alpha=1}$ via (3);
(c) compute the coarse frequency estimate $\hat{f}_d^{c1}$ by means of (5), and update $\hat{f}_d^c$ as $\hat{f}_d^{c1}$;
(d) compensate $z(k)$ by $\hat{f}_d^c$ and obtain the corrected one $z_1(k)$;
(e) compute the other coarse frequency estimate $\hat{f}_d^{c2}$ through (6), and update $\hat{f}_d^c$ as $\hat{f}_d^{c1} + \hat{f}_d^{c2}$.

3.2 Fine Frequency Estimation

In the fine frequency estimation, we use the received signals corresponding to the multiple disjoint pilot blocks to obtain more precise frequency estimate.

With loss of generality, the equilibrium of all the pilot blocks is considered except the first pilot block, i.e. $L_i \equiv L$. A so-called cross- correlation operation is carried out as follows

$$\begin{aligned} R_c(i) &= \sum_{k=0}^{L-1} z_2^*(k) z_2(k + D_i), \\ D_i &= \sum_{j=1}^{i} (L_j + M_j),\ i = 1, 2, \ldots, N-1 \end{aligned} \tag{8}$$

for each $R_c(i)$, we can obtain a fine frequency estimate (or say residual frequency estimate) via taking the argument of (8), i.e.

$$\hat{f}_d^{fi} = \frac{1}{2\pi T D_i} \arg\{R_1(i)\}. \tag{9}$$

So far, a final frequency estimate can be derived as combining (5), (6) and (9)

$$\hat{f}_d = \hat{f}_d^c + \hat{f}_d^f = \hat{f}_d^{c1} + \hat{f}_d^{c2} + \sum_{i=1}^{N-1} \hat{f}_d^{fi}. \tag{10}$$

Similarly, the fine frequency estimator can be summarized as follows:

Initialization: set $i = 0$, $\hat{f}_d^{i0} = 0$ and $k \in \kappa$.

(a) compensate the removed-modulation signal $z(k)$ by $\hat{f}_d^c$;
(b) get the cross-correlation value $R_c(i)$ by (8);
(c) if $i = N - 1$, stop and update the fine frequency estimate $\hat{f}_d^f$ as $\sum_{i=1}^{N-1} \hat{f}_d^{fi}$, otherwise go to the next step;

(d) let $i = i + 1$, compute the i-th fine frequency estimate value $\hat{f}_d^{fi}$ through (9) and go to the step b.

After the frequency estimation, the following phase estimation can be executed based on the maximum likelihood (ML) criterion, which is given in detail in [15].

3.3 Compensator

After the frequency estimation and the phase offset estimation, the estimates $\hat{f}_d$ and $\hat{\theta}$ are obtained. The following compensator (COM) will apply the two estimates into the received data signals $\{r_d(k)\}$ i.e.

$$\tilde{r}_d(k) = r_d(k)\exp\left[-j\left(2\pi\hat{f}_d kT + \hat{\theta}\right)\right] \tag{11}$$

The summarized process of our proposed carrier synchronizator is shown in Fig. 3.

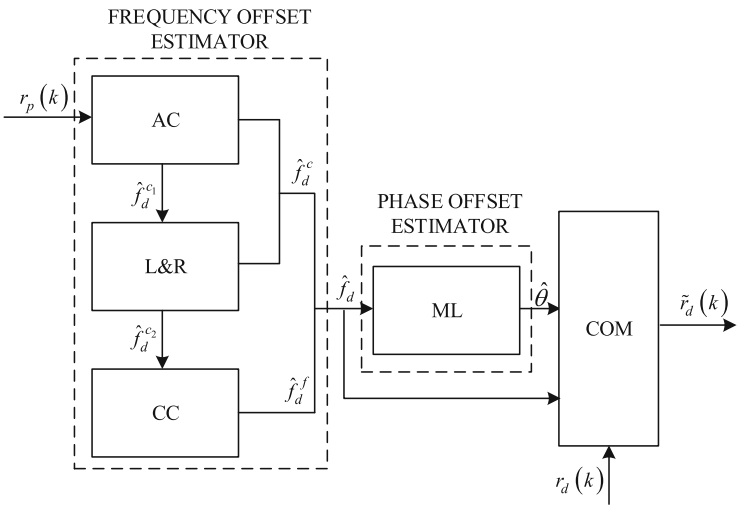

Fig. 3. The proposed carrier synchronizator

4 Simulation Results

In this section, we will evaluate both the estimation accuracy and bit-error-rate (BER) performance of the proposed carrier synchronizator.

Consider a (225,173) nonbinary LDPC code over GF(16) and 16-QAM system. Without loss of generality, we divide the coded modulation signals into two blocks: $M_1 = 113$ and $M_2 = 112$. The lengths of corresponding pilot blocks are L_1, L_2 and L_3 ($L_2 = L_3$), respectively. Thus, the resulting pilot overhead can be defined as η with the form of

$$\begin{aligned}\eta &= \frac{L_1 + L_2 + L_3}{L_1 + L_2 + L_3 + M_1 + M_2} \times 100\% \\ &= \frac{L_1 + 2L_2}{L_1 + 2L_2 + 225} \times 100\%.\end{aligned} \tag{12}$$

We take three pilot block lengths for examples, followed by three corresponding pilot overheads listed in Table 1.

Table 1. The pilot lengths and corresponding pilot overheads.

L_1	L_2	L_3	η
20	3	3	10%
20	10	10	15%
27	15	15	20%

4.1 Analysis of Estimation Accuracy

In this part, we will analyze performance of both the frequency and phase offset estimation of the proposed carrier synchronizator, followed by corresponding Cramer-Rao bounds (CRBs).

Based on our previous work [14], the CRBs for frequency offset and phase offset can be expressed as respectively

$$\begin{aligned}\mathrm{CRB}(f_d)^{-1} = \frac{C}{6}\sum_{i=1}^{N} L_i(L_i-1)(2L_i-1) + C\sum_{i1=2}^{N} L_{i1}\sum_{i2=1}^{i1}(L_{i2}+M_{i2})\cdot \\ \left[\sum_{i2=1}^{i1}(L_{i2}+M_{i2}) + L_{i1} - 1\right]\end{aligned} \tag{13}$$

$$\mathrm{CRB}(\theta)^{-1} = 2L_1 \times \frac{E_s}{N_0} \tag{14}$$

where the coefficient $C \triangleq 8\pi^2 T^2 E_s/N_0$. It is seen that for a DA synchronizator, both the CRBs will become lower with an increase of the SNR and/or the pilot block length.

Figure 4 shows frequency and phase offset estimation along with corresponding CRBs when $f_d T = 0.3$ and $\theta = \pi/2$. As shown in Fig. 4(a): if using 20% pilot overhead, the proposed synchronizator can achieve good accuracy extremely close to its CRB only at 3 dB. But if using fewer pilots overhead, the corresponding accuracy will deteriorate sharply. In Fig. 4(b), if using 20% pilot overhead, the proposed synchronizator can also achieve good accuracy very close to its CRB. Further, the achievable estimation accuracy of the proposed synchronizator depends on its BER performance.

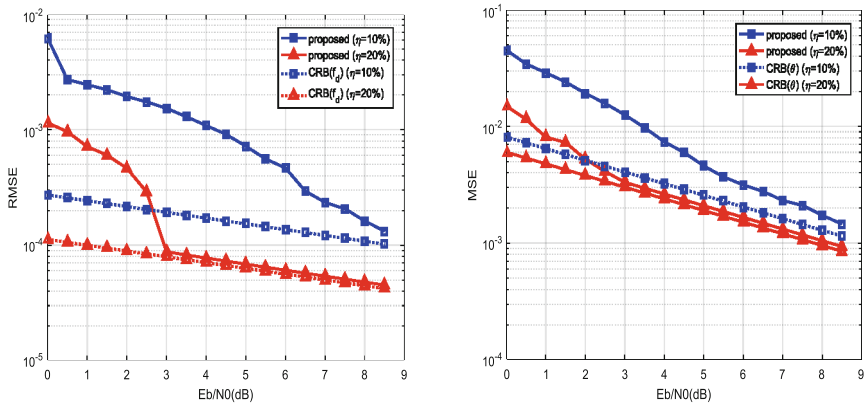

(a) Frequency offset estimation versus its CRB (b) Phase offset estimation versus its CRB

Fig. 4. Evaluation of the frequency and phase offset estimation along with the corresponding CRBs

4.2 Analysis of BER Performance

According to the above discussions, Fig. 5 shows BER performance of the proposed carrier synchronizator under the conditions of $f_dT = 0.3$ and $\theta = \pi/2$. It is seen that at a BER of 10^{-5}, the proposed carrier synchronizator using the 20% pilot overhead can obtain good performance which is 1.2 dB away from the ideal performance ($f_d = 0$ and $\theta = 0$); at a BER of 10^{-4}, the proposed carrier synchronizator using the 20% and 15% pilot overheads can achieve good performance (only 0.8 dB and 1.6 dB away from the ideal performance respectively). For less pilot overhead (e.g. 10%), the performance of our proposed carrier synchronizator will deteriorate sharply, which corresponds to the results of Fig. 4.

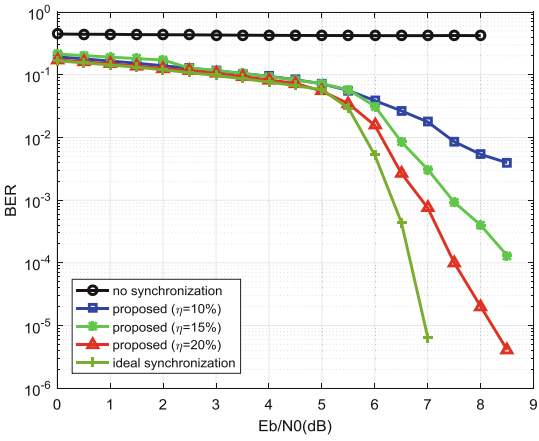

Fig. 5. Evaluation of BER performance of the proposed carrier synchronizator

5 Conclusions

Considering large Doppler shift, random phase offset and low spectrum efficiency in the satellite communication, we propose a carrier synchronizator in nonbinary LDPC and high-order QAM system. Based on the system, large Doppler shift can be eliminated by a single pilot block-aided joint AC and L&R algorithm and a multiple pilot block-aided CC algorithm. Also, random phase offset can be removed by using a single pilot block-aided ML algorithm. Simulation result shows that for a (225,173) nonbinary LDPC over GF(16) and 16-QAM system, our proposed carrier synchronizator can achieve good performance in both the RMSE/MSE and BER as the pilot overhead increases.

Acknowledgment. This work was supported in part by the National Natural Science Foundation of China, by the 973 Program of China under Grants 61372074 and 91438101 and 2012CB316103, by the Fundamental Research Funds for the Central Universities (JBG160103, XJS15019), and by the China Postdoctoral Science Foundation funded project (2015M580819).

References

1. Silva, J.S., et al.: Stereolithography-based antennas for satellite communications in Ka-Band. Proc. IEEE **105**(4), 655–667 (2017)
2. Joroughi, V., et al.: Generalized multicast multibeam precoding for satellite communications. IEEE Trans. Wirel. Commun. **16**(2), 952–966 (2017)
3. Meng, X., et al.: A DS-PAM UWB TT&C signal improvement method. In: 2016 IEEE 13th International Conference on Signal Processing, pp. 1157–1160 (2016)
4. Wang, W.-Q.: Carrier frequency synchronization in distributed wireless sensor networks. IEEE Syst. J. **9**(3), 703–713 (2015)
5. Zibar, D., et al.: Joint iterative carrier synchronization and signal detection employing expectation maximization. J. Lightwave Technol. **32**(8), 1608–1615 (2014)
6. Sun, J., Yu, Z., et al.: Simplified diagonal cross-correlation frequency estimation based on phase un-wrapping. In: 2015 10th International Conference on Communications and Networking in China (ChinaCom), Shanghai, pp. 739–744 (2015)
7. Moeneclaey, M., de Jonghe, G.: ML-oriented NDA carrier synchronization for general rotationally symmetric signal constellations. IEEE Trans. Commun. **42**(8), 2531–2533 (1994)
8. Luise, M., Reggiannini, R.: Carrier frequency recovery in all-digital modems for burst-mode transmissions. IEEE Trans. Commun. **43**(2), 1169–1178 (1995)
9. Godtmann, S., Hadaschik, N., Steinert, W., et al.: A concept for data-aided carrier frequency estimation at low signal-to-noise ratio. In: Proceeding of 2008 IEEE International Conference on Communications (ICC), Beijing, China, pp. 463–467 (2008)
10. Man, X., et al.: A novel code-aided carrier recovery algorithm for coded systems. IEEE Commun. Lett. **17**(2), 405–408 (2013)
11. Nele, N., Heidi, S., Moeneclaey, M.: Carrier phase tracking from turbo and LDPC coded signals affected by a frequency offset. IEEE Commun. Lett. **9**(10), 915–917 (2005)
12. Gallager, R.G.: Low-density parity-check codes. IRE Trans. Inf. Theory **8**(1), 21–28 (1962)

13. MacKay, D.J.C., Neal, R.M.: Near Shannon limit performance of low-density parity-check codes. IEEE Electron Lett. **33**(6), 457–458 (1997)
14. Yu, Z., Sun, J., Bai, B., et al.: A phase increment-based frequency estimator for general PSAM in burst communications. In: 2016 IEEE 83rd Vehicular Technology Conference (VTC Spring), Nanjing, pp. 1–5 (2016)
15. Wang, P.S., Lin, D.W.: On maximum-likelihood blind synchronization over WSSUS channels for OFDM systems. IEEE Trans. Signal Process. **63**(19), 5045–5059 (2015)